

# Implications of percolation of colour strings on multiplicities, correlations and the transverse momentum

M.A.Braun

High-energy physics department  
S.Petersburg University, 198904 S.Petersburg, Russia  
and C.Pajares

Departamento de Física de Partículas,  
Universidade de Santiago de Compostela,  
15706-Santiago de Compostela, Spain

July 1999

Percolation, multiplicities,  $\langle p_T^2 \rangle$  and correlations.

## Abstract.

In the colour string model the impact of string percolation on multiplicities,  $\langle p_T^2 \rangle$  and their long range (forward-backward) correlations is studied. It is assumed that different string overlaps produce the observed hadrons independently. The multiplicities are shown to be damped by a simple factor which follows from the percolation theory. The  $\langle p_T^2 \rangle$  rise at the same rate as multiplicities fall. A clear signature of the percolation phase transition is found to be a behaviour of the forward-backward correlations for intensive quantities, such as  $\langle p_T^2 \rangle$  or its inverse, which can be detected in the relativistic heavy ion collider.

**hep-ph/9907332**  
**US-FT/15-99**

# 1 Introduction

Multiparticle production at high energies is currently (and successfully) described in terms of colour strings stretched between the projectile and target [1-6]. Hadronization of these strings produces the observed hadrons. Colour strings may be viewed upon as (small) areas in the transverse space filled with colour field created by the colliding partons. Creation of particles goes via emission of  $q\bar{q}$  pairs in this field. With growing energy and/or atomic number of colliding particles, the number of strings grows. Once strings have a certain nonzero dimension in the transverse space they start to overlap forming clusters, very much like disks in the 2-dimensional percolation theory. The geometrical behaviour of strings in the transverse plane then follows that of percolating discs. In particular at a certain critical string density a macroscopic cluster appears (infinite in the thermodynamic limit), which marks the percolation phase transition [7 - 9].

The percolation theory governs the geometrical pattern of the string clustering. Its observable implications however require introduction of some dynamics to describe string interaction, that is, the behavior of a cluster formed by several overlapping strings.

One can study different possibilities.

A most naive attitude is to assume that nothing happens as strings overlap, in other words, they continue to emit particles independently without being affected by their overlapping neighbours. This is a scenario of non-interacting strings, which closely corresponds to original calculations in the colour strings approach, oriented at comparatively small energies (and numbers of strings). This scenario however contradicts the idea that strings are areas of the transversal space filled with colour field and thus with energy, since in the overlapping areas the energy should have grown.

In another limiting case one may assume that a cluster of several overlapping strings behaves as a single string with an appropriately higher colour field (a string of higher colour, or a "colour rope" [10]). This fusion scenario was proposed by the authors and later realized as a Monte-Carlo algorithm nearly a decade ago [11,12]. It predicts lowering of total multiplicities and forward-backward correlations (FBC) and also strange baryon enhancement, in a reasonable agreement with the known experimental trends.

However both discussed scenarios are obviously of a limiting sort. In a typical situation strings only partially overlap and there is no reason to expect them to fuse into a single stringy object, especially if the overlap is small. The transversal space occupied by a cluster of overlapping strings splits into a number of areas in which different number of string overlap, including areas where no overlapping takes place. In each such area colour fields coming from the overlapping strings will add together. As a result the total cluster area is split in domains with different colour field strength. As a first approximation, neglecting the interaction at the domain frontiers, one may assume that emission of  $q\bar{q}$  pairs in the domains proceeds independently, governed by the field strength ("the string tension") in a given domain. This picture implies that clustering of strings actually leads to their proliferation, rather than fusion, since each particular overlap may be considered as a separate string. Evidently newly formed strings differ not only in their colours but also in their transverse areas.

As a simple example consider a cluster of two partially overlapping strings (Fig. 1). One distinguishes three different regions: regions 1 and 2 where no overlapping takes

place and the colour field remains the same as in a single string, and the overlap region 3 with colour fields of both strings summed. In our picture particle production will proceed independently from these three areas, that is, from three different "strings" corresponding to areas 1,2 and 3. In this sense string interaction has split two strings into three of different colour, area and form in the transverse space.

We stress that these dynamical assumptions are rather independent of the geometrical picture of clusterization. In particular, in each of the scenarios discussed above, at a certain string density there occurs the percolation phase transition. However its experimental signatures crucially depend on the dynamical contents of string interaction. With no interaction, clustering does not change physical observables, so that the geometric percolation will not be felt at all. With the interaction between strings turned on, clustering (and percolation) lead to well observable implications.

In this note we shall study these implications for simplest observables, such as multiplicities, average transverse momenta and FBC in the realistic scenario discussed above, which corresponds to independent particle production from different overlap domains. Our choice of observables is dictated by the possibility to relate them directly to the domain properties, without introducing any more assumptions.

## 2 Multiplicity and $\langle p_T^2 \rangle$ for overlapping strings

As stated in the Introduction, the central dynamical problem is to find how the observables change when several strings form a cluster partially overlapping. In the overlap areas the colour fields of individual strings are summed together. It is more convenient to sum the charges which generate the colour field of overlapping strings.

Let only two strings, of areas  $\sigma_0$  in the transverse space each, partially overlap in the area  $S_2$  (region 3 in Fig. 1), so that  $S_1 = \sigma_0 - S_2$  is the area in each string not overlapping with the other. In the following it will be called the overlap area of one string. A natural assumption seems to be that the average colour density  $\xi$  of the string in the transverse plane is a constant

$$\xi = Q_0/\sigma_0, \quad (1)$$

where  $Q_0$  is a color of the string. For partially overlapping strings the colour in each of the two non-overlapping areas will then be

$$Q_1 = \xi S_1 = Q_0(S_1/\sigma_0). \quad (2)$$

The colour in the overlap area  $Q_2$  will be a vector sum of the two overlapping colours  $\xi S_2$ . In this summation the total colour squared should be conserved [10]. Indeed,  $Q_2^2 = (\mathbf{Q}_{ov} + \mathbf{Q}'_{ov})^2$  where  $\mathbf{Q}_{ov}$  and  $\mathbf{Q}'_{ov}$  are the two vector colours in the overlap area. Since the colours in the two strings may generally be oriented in an arbitrary manner respective to one another, the average of  $\mathbf{Q}_{ov} \mathbf{Q}'_{ov}$  is zero. Then  $Q_2^2 = Q_{ov}^2 + Q'_{ov}{}^2$ , which leads to

$$Q_2 = \sqrt{2} \xi S_2 = \sqrt{2} Q_0(S_2/\sigma_0). \quad (3)$$

One observes that, due to its vector nature, the colour in the overlap is less than the sum of the two overlapping colours. This phenomenon was first mentioned in [10] for the so-called colour ropes.

Two simplest observables, the multiplicity  $\mu$  and the average transverse momentum squared  $\langle p_T^2 \rangle$  are directly related to the field strength in the string and thus to its generating colour. In fact they are both proportional to the colour [10,13]. Thus, assuming independent emission from the three regions 1,2 and 3 in Fig. 1 we get for the multiplicity

$$\mu/\mu_0 = 2(S_1/\sigma_0) + \sqrt{2}(S_2/\sigma_0), \quad (4)$$

where  $\mu_0$  is a multiplicity for a single string. To find  $\langle p_T^2 \rangle$  one has to divide the total transverse momentum squared of all observed particles by the total multiplicity. In this way for our cluster of two strings we obtain

$$\langle p_T^2 \rangle / \langle p_T^2 \rangle_0 = \frac{2(S_1/\sigma_0) + \sqrt{2}\sqrt{2}(S_2/\sigma_0)}{2(S_1/\sigma_0) + \sqrt{2}(S_2/\sigma_0)} = \frac{2}{2(S_1/\sigma_0) + \sqrt{2}(S_2/\sigma_0)}, \quad (5)$$

where  $\langle p_T^2 \rangle_0$  is the average transverse momentum squared for a single string and we have used the evident property  $2S_1 + 2S_2 = 2\sigma_0$  in the second equality.

Generalizing to any number  $N$  of overlapping strings we find the total multiplicity as

$$\mu/\mu_0 = \sum_i \sqrt{n_i} (S^{(i)}/\sigma_0), \quad (6)$$

where the sum goes over all individual overlaps  $i$  of  $n_i$  strings having areas  $S^{(i)}$ . Similarly for the  $\langle p_T^2 \rangle$  we obtain

$$\langle p_T^2 \rangle / \langle p_T^2 \rangle_0 = \frac{\sum_i n_i (S^{(i)}/\sigma_0)}{\sum_i \sqrt{n_i} (S^{(i)}/\sigma_0)} = \frac{N}{\sum_i \sqrt{n_i} (S^{(i)}/\sigma_0)}. \quad (7)$$

In the second equality we again used an evident identity  $\sum_i n_i S^{(i)} = N\sigma_0$ . Note that (6) and (7) imply a simple relation between the multiplicity and transverse momentum

$$\frac{\mu}{\mu_0} \frac{\langle p_T^2 \rangle}{\langle p_T^2 \rangle_0} = N, \quad (8)$$

which evidently has a meaning of conservation of the total transverse momentum produced.

Eqs. (6) and (7) do not look easy to apply. To calculate the sums over  $i$  one seems to have to identify all individual overlaps of any number of strings with their areas. For a large number of strings the latter may have very complicated forms and their analysis presents great calculational difficulties. However one immediately recognizes that such individual tracking of overlaps is not at all necessary. One can combine all terms with a given number of overlapping strings  $n_i = n$  into a single term, which sums all such overlaps into a total area of exactly  $n$  overlapping strings  $S_n$ . Then one finds instead of (6) and (7)

$$\mu/\mu_0 = \sum_{n=1}^N \sqrt{n} (S_n/\sigma_0) \quad (9)$$

and

$$\langle p_T^2 \rangle / \langle p_T^2 \rangle_0 = \frac{N}{\sum_{n=1}^N \sqrt{n} (S_n/\sigma_0)}. \quad (10)$$

In contrast to individual overlap areas  $S^{(i)}$  the total ones  $S_n$  can be easily calculated (see Appendix). Let the projections of the strings onto the transverse space be distributed uniformly in the interaction area  $S$  with a density  $\rho$ . Introduce a dimensionless parameter

$$\eta = \rho\sigma_0 = N\sigma_0/S. \quad (11)$$

The "thermodynamic limit" corresponds to taking the number of the strings  $N \rightarrow \infty$  keeping  $\eta$  fixed. In this limit one readily finds that the distribution of the overlaps of  $n$  strings is Poissonian with a mean value  $\eta$ :

$$p_n = \frac{S_n}{S} = \frac{\eta^n}{n!} e^{-\eta}. \quad (12)$$

From (9) we then find that the multiplicity is damped due to overlapping by a factor

$$F(\eta) = \frac{\mu}{N\mu_0} = \frac{\langle \sqrt{n} \rangle}{\eta}, \quad (13)$$

where the average is taken over the Poissonian distribution (12).

The behaviour of  $F(\eta)$  is shown in Fig. 2. It smoothly goes down from unity at  $\eta = 0$  to values around 0.5 at  $\eta = 4$  falling as  $1/\sqrt{\eta}$  for larger  $\eta$ 's. According to (10) the inverse of  $F$  shows the rise of the  $\langle p_T^2 \rangle$ . Note that a crude estimate of  $F(\eta)$  can be done from the overall compression of the string area due to overlapping. The fraction of the total area occupied by the strings according to (12) (see also [14]) is given by

$$\sum_{n=1} p_n = 1 - e^{-\eta}. \quad (14)$$

The compression is given by (14) divided by  $\eta$ . According to our picture the multiplicity is damped by the square root of the compression factor, so that the damping factor is

$$F(\eta) = \sqrt{\frac{1 - e^{-\eta}}{\eta}}. \quad (15)$$

For all the seeming crudeness of this estimate, (15) is very close to the exact result, as shown in Fig. 2 by a dashed curve.

### 3 Percolation

Percolation is a purely classical mechanism. Overlapping strings form clusters. At some critical value of the parameter  $\eta$  a phase transition of the 2nd order occurs: a cluster appears which extends over the whole surface (an infinite cluster in the thermodynamic limit). The critical value of  $\eta$  is found to be  $\eta_c \simeq 1.12 - 1.20$  [15]. Below the phase transition point, for  $\eta < \eta_c$ , there is no infinite cluster, Above the transition point, at  $\eta > \eta_c$  an infinite cluster appears with a probability

$$P_\infty = \theta(\eta - \eta_c)(\eta - \eta_c)^\beta. \quad (16)$$

The critical exponent  $\beta$  can be calculated from Monte-Carlo simulations. However the universality of critical behaviour, that is, its independence of the percolating substrate, allows to borrow its value from lattice percolation, where  $\beta = 5/36$ .

Cluster configuration can be characterized by the occupation numbers  $\langle \nu_n \rangle$ , that is average numbers of clusters made of  $n$  strings. Their behaviour at all values of  $\eta$  and  $n$  is not known. From scaling considerations in the vicinity of the phase transition it has been found [24]

$$\langle \nu_n \rangle = n^{-\tau} F(n^\sigma(\eta - \eta_c)), \quad |\eta - \eta_c| \ll 1, \quad n \gg 1, \quad (17)$$

where  $\tau = 187/91$  and  $\sigma = 36/91$  and the function  $F(z)$  is finite at  $z = 0$  and falls off exponentially for  $|z| \rightarrow \infty$ . Eq. (17) is of limited value, since near  $\eta = \eta_c$  the bulk of the contribution is still supplied by low values of  $n$ , for which (14) is not valid. However from (17) one can find non-analytic parts of other quantities of interest at the transition point. In particular, one finds a singular part of the total number of clusters  $M = \sum \nu_n$  as  $\Delta \langle M \rangle = c|\eta - \eta_c|^{8/3}$ . This singularity is quite weak: not only  $\langle M \rangle$  itself but also its two first derivatives in  $\eta$  stay continuous at  $\eta = \eta_c$  and only the third blows up as  $|\eta - \eta_c|^{-1/3}$ . So one should not expect that the percolation phase transition will be clearly reflected in some peculiar behaviour of standard observables.

Indeed we observed that neither the total multiplicity nor  $\langle p_T^2 \rangle$  show any irregularity in the vicinity of the phase transition, that is, at  $\eta$  around unity. This is not surprising since both quantities reflect the overlap structure rather than the cluster one. The connectedness property implied in the latter has no effect on these global observables.

It is remarkable, however, that the fluctuations of these observables carry some information about the phase transition. The dispersion of the multiplicity due to overlapping and clustering can easily be calculated in the thermodynamic limit (see Appendix). The result is shown in Fig. 3. The dispersion shows a clear maximum around  $\eta = 1$  (in fact at  $\eta \simeq 0.7$ ). So some information of the percolation phenomenon is passed to the total multiplicity, in spite of the fact that it basically does not feel the connectedness properties of the formed clusters. Of course, due to relation (10), the dispersion of  $\langle p_T^2 \rangle$  has a similar behaviour.

We have to warn against a simplistic interpretation of this result. The dispersion shown in Fig. 3 is only part of the total one, which besides includes contributions from the fluctuations inside the strings and also in their number. Below we shall discuss the relevance and magnitude of these extra contributions.

An intriguing question is a relation between the percolation and formation of the quark-gluon plasma. Formally these phenomena are different. Percolation is related to the connectedness property of the strings. The (cold) quark-gluon plasma formation is related to the density of the produced particles (or, equivalently, the density of their transverse energy). However in practice percolation and plasma formation go together. In fact, the transverse energy density inside a single string seems to be sufficient for the plasma formation. Percolation makes the total area occupied by strings comparable to the total interaction area, thus, creating, a sizable area with energy densities above the plasma formation threshold.

Let us make some crude estimates. Comparison with the observed multiplicity densities in  $pp(\bar{p})$  collisions at present energies fix the number of produced (charged) particles per string per unit rapidity at approximately unity. Taking the average energy of each particle as 0.4 GeV (which is certainly a lower bound), formation length in the Bjorken formula [16] as 1 fm and the string transverse radius as 0.2 fm [7] we get the 3-dimensional transverse energy density inside the string as  $\sim 3 \text{ GeV}/\text{fm}^3$ . The plasma threshold is currently estimated to be at  $1 \text{ GeV}/\text{fm}^3$ . So it is tempting to say that the

plasma already exists inside strings. This however has little physical sense because of a very small area occupied by a string. One can speak of a plasma only when the total area occupied by a cluster of strings reaches a sizable fraction of the total interaction area. In Fig. 4 we show this fraction for a maximal cluster as a function of  $\eta$  calculated by Monte -Carlo simulations in a system of 50 strings. It grows with  $\eta$  and the fastest growth occurs precisely in the region of the percolation phase transition: as  $\eta$  grows from 0.8 to 1.2 the fraction grows from 0.3 to 0.6. With a string cluster occupying more than half of the interacting area, one can safely speak of a plasma formed in that area.

## 4 Dispersions and forward-backward correlations

As shown in the previous section a definite signal for the percolation phase transition comes from the multiplicity (or  $\langle p_T^2 \rangle$ ) fluctuations due to string clustering. However these fluctuations are not the only ones. An important contribution also comes from the fluctuations of the multiplicity inside the strings, or rather inside the individual overlaps of strings, which in our picture play the role of independent particle emitters. To find the total dispersion it is convenient to use a formalism of the generating functions. Let the total probability to observe  $n$  produced particles be  $\mathcal{P}(n)$ . In our picture it is given by a convolution of the probability for a given overlap configuration  $P(C)$  with the probabilities for particle production from all individual overlaps:

$$\mathcal{P}(n) = \sum_C P(C) \sum_{n_1, \dots, n_M} p_1(n_1) \dots p_M(n_M) \delta_{n, \sum n_i}. \quad (18)$$

Here  $C$  is a "configuration", characterized by the total number of the overlaps  $M$  and their individual properties: area and number of overlapping strings. We pass to generating functions

$$\Phi(z) = \sum_n z^n \mathcal{P}(n), \quad \phi_i(z) = \sum_n z^n p_i(n), \quad (19)$$

for which (18) transforms into

$$\Phi(z) = \sum_C P(C) \prod_i \phi_i(z). \quad (20)$$

The overall averages (with the probability  $\mathcal{P}$ ) are given by

$$\langle n \rangle = \Phi'(z)_{z=1}, \quad \langle n(n-1) \rangle = \Phi''(z)_{z=1}. \quad (21)$$

The averages inside the  $i$ -th overlap are likewise given by

$$\bar{n}_i = \phi_i'(z)_{z=1}, \quad \overline{n_i(n_i-1)} = \phi_i''(z)_{z=1}. \quad (22)$$

Using this formulas one readily finds the total dispersion of multiplicity as a sum of two terms

$$D^2 = D_C^2 + D_{in}^2. \quad (23)$$

Here  $D_C^2$  is a dispersion due to fluctuation in configurations

$$D_C^2 = \sum_C P(C) \sum_{ik} \bar{n}_i \bar{n}_k - \left( \sum_C P(C) \sum_i \bar{n}_i \right)^2. \quad (24)$$

It is calculated according to the distribution  $\mathcal{P}$  assuming that the numbers of particles produced in individual overlaps are fixed to be their averages. It is this part of the dispersion, which is calculated in the Appendix and presented in Fig.3. The part  $D_{in}^2$  is a part of the dispersion due to fluctuations inside the individual overlaps:

$$D_{in}^2 = \sum_C P(C) \sum_i (\overline{n_i^2} - (\overline{n_i})^2). \quad (25)$$

Its calculation is extremely difficult even in by Monte Carlo simulations, since it requires identification of all individual overlaps and knowledge of their areas. To simplify we assume that the distribution of produced particles from any overlap is Poissonian, so that  $\overline{n_i^2} - (\overline{n_i})^2 = \overline{n_i}$ . Then we evidently find

$$D_{in}^2 = \mu. \quad (26)$$

From the experimental data we estimate  $\mu_0 \simeq 1.1$  for unit rapidity interval. Comparison of Fig.2 and Fig. 3 then shows that for unit rapidity interval the internal dispersion  $D_{in}^2$  is roughly 40 times greater than the "percolation dispersion"  $D_C^2$  at  $\eta = 0.7$  corresponding to the maximum for the latter. At other  $\eta$  the ratio  $D_{in}^2/D_C^2$  is still greater. With the growth of the rapidity interval this ratio diminishes proportionally. However it is obvious that one should not expect to clearly see the percolation effects directly in the observed multiplicities.

A better signal for the percolation comes from the FBC, which, as we shall see, distinguish between the percolation and intrinsic dispersions (in fact they depend on their ratio). The FBC are described by the dependence of the average multiplicity in the backward hemisphere  $\langle \mu_B \rangle$  on the event multiplicity in the forward hemisphere  $\mu_F$ . The data can be fitted by a linear expression [1]

$$\langle \mu_B \rangle = a + b\mu_F, \quad (27)$$

where  $a$  and  $b$  are given by expectation values

$$a = \frac{\langle \mu_B \rangle \langle \mu_F^2 \rangle - \langle \mu_F \mu_B \rangle \langle \mu_F \rangle}{\langle \mu_F^2 \rangle - \langle \mu_F \rangle^2}, \quad (28)$$

$$b = \frac{\langle \mu_F \mu_B \rangle - \langle \mu_F \rangle \langle \mu_B \rangle}{\langle \mu_F^2 \rangle - \langle \mu_F \rangle^2}. \quad (29)$$

In absence of FBC  $\langle \mu_F \mu_B \rangle = \langle \mu_F \rangle \langle \mu_B \rangle$  and one obtains  $a = \langle \mu_F \rangle$  and  $b = 0$ . So the strength of the correlations is given by the coefficient  $b$ .

To calculate the necessary averages we introduce the probability  $\mathcal{P}(F, B)$  to produce  $F(B)$  particles in the forward (backward) hemispheres. Similar to (18) it is given by a convolution

$$\mathcal{P}(F, B) = \sum_C P(C) \sum_{F_i, B_i} \prod_i p_i(F_i, B_i) \delta_{F, \sum F_i} \delta_{B, \sum B_i}, \quad (30)$$

which transforms into a relation between the generating functions

$$\Phi(z_F z_B) = \sum_C P(C) \prod_i \phi(z_F, z_B). \quad (31)$$



Instead of (21) we now have

$$\langle F \rangle = \left( \frac{\partial \Phi}{\partial z_F} \right)_{z_F=z_B=1}, \quad \langle F(F-1) \rangle = \left( \frac{\partial^2 \Phi}{\partial z_F^2} \right)_{z_F=z_B=1}, \quad \langle FB \rangle = \left( \frac{\partial^2 \Phi}{\partial z_F \partial z_B} \right)_{z_F=z_B=1}, \quad (32)$$

formulas similar to the first two for  $B$ , and similar formulas for the averages over the distributions  $p_i$  inside the overlap  $i$  with the generating function  $\phi_i(z_F, z_B)$ . Using this formulas we find that the dispersions again split into the percolation (C) and internal (in) parts.

$$D_F^2 = D_{F,C}^2 + D_{F,in}^2, \quad D_{FB}^2 \equiv \langle FB \rangle - \langle F \rangle \langle B \rangle = D_{FB,C}^2 + D_{FB,in}^2. \quad (33)$$

They are given by

$$D_{F,C}^2 = \sum_C P(C) \sum_{i,k} \bar{F}_i \bar{F}_k - \left( \sum_C P(C) \sum_i \bar{F}_i \right)^2, \quad (34)$$

$$D_{FB,C}^2 = \sum_C P(C) \sum_{i,k} \bar{F}_i \bar{B}_k - \sum_C P(C) \sum_i \bar{F}_i \sum_C P(C) \sum_i \bar{B}_i, \quad (35)$$

$$D_{F,in}^2 = \sum_C P(C) \sum_i (\bar{F}_i^2 - (\bar{F}_i)^2), \quad (36)$$

$$D_{FB,in}^2 = \sum_C P(C) \sum_i (\bar{F}_i \bar{B}_i - \bar{F}_i \bar{B}_i). \quad (37)$$

The usual assumption is that there are no FB correlations for particle production from a single emitter (overlap  $i$  in our case). Then  $D_{FB,in}^2 = 0$ . Also from  $n = F + B$  one can relate these dispersions with the overall ones  $D_C^2$  and  $D_{in}^2$ :

$$D_{F,C}^2 = D_{FB,C}^2 = (1/4)D_C^2, \quad D_{F,in}^2 = (1/2)D_{in}^2. \quad (38)$$

From (29) one then finds

$$\frac{1}{b} = 1 + 2 \frac{D_{in}^2}{D_C^2}. \quad (39)$$

So, the FBC parameter  $b$  indeed measures the ratio of internal to percolation dispersions squared. If we assume that the distribution of particles produced from an individual overlap is Poissonian then (39) transforms into

$$\frac{1}{b} = 1 + 2 \frac{\mu}{D_C^2}. \quad (40)$$

Both  $\mu$  and  $D_C^2$  grow linearly with the number of strings  $N$ , so in the thermodynamic limit  $b$  does not depend on  $N$ . However it depends on the multiplicity of a single string  $\mu_0$ , since  $\mu$  is proportional to  $\mu_0$  and  $D_C^2$  is proportional to  $\mu_0^2$ . As mentioned, from the experimental data we find that  $\mu_0 \simeq 1.1y$  where  $y$  is the rapidity interval of the produced particles. So the right-hand side of (40) falls with the growth of the rapidity window. It also has a minimum at  $\eta \sim 0.7$  corresponding to the maximum  $D_C^2$ . From this we see that the FBC parameter  $b$  also has a maximum near  $\eta \sim 0.7$  whose magnitude grows with the rapidity interval. In Fig. 5 we show the behaviour of  $b$  as a function of  $\eta$  for two rapidity intervals  $y = 5$  and  $y = 9$

One can also study the FBC for  $\langle p_T^2 \rangle$ . Due to relation (8), for fixed  $N$  they are uniquely determined by the fluctuations in  $\mu$ . It is convenient to choose the inverse  $\langle p_T^2 \rangle$  as an observable:

$$\tau = \frac{\mu_0 \langle p_T^2 \rangle_0}{\langle p_T^2 \rangle} = \frac{\mu}{N}. \quad (41)$$

Then it is obvious that the parameter  $b$  for  $\tau$  is the same as for the multiplicity, since both percolation and internal dispersions for  $\tau$  are obtained from those for  $\mu$ , divided by  $N$ . However this equivalence holds only for fixed number of strings  $N$ . In the realistic situation  $N$  fluctuates. The multiplicity is an extensive observable and carries these fluctuations directly. They result large and smear out nearly all traces of percolation. In contrast,  $\tau$  is an intensive observable and so feels the fluctuation in  $N$  only indirectly, through the fluctuations in the parameter  $\eta$ . As a result, the percolation effects for the FBC in  $\tau$  are clearly visible, as we shall see in the next section.

## 5 Realistic hadronic and nuclear collisions

For realistic hadronic and nuclear collisions the total number of strings  $N$  grows with energy and fluctuates. For pp collisions the initial number of colour strings  $N$  created at a given c.m. energy  $\sqrt{s}$  can be taken from the well-known calculations of [1,2]. For pA and AB collisions this number should be multiplied by the effective number of collisions  $C$ . At asymptotic energies for minimum bias hA and AB collisions the AGK rules predict

$$C_A = A\sigma/\sigma_A, \quad C_{AB} = AB\sigma/\sigma_{AB}, \quad (42)$$

where  $\sigma$  ( $\sigma_A$ ,  $\sigma_{AB}$ ) is the inelastic pp (pA, AB) cross-section. For hA collisions at fixed impact parameter  $b$

$$C_A = A\sigma T_A(b)/(1 - \exp(-A\sigma T_{AB})), \quad (43)$$

where  $T_A$  is the standard nuclear profile function (normalized to unity). The same relation holds for AB collisions in the optical approximation with

$$A \rightarrow AB, \quad T_A \rightarrow T_{AB}(b) = \int d^2c T_A(c) T_B(b-c). \quad (44)$$

The transverse interaction area for pp and hA collisions obviously is of the order  $\sigma$ . For AB collisions it depends on the geometry of the collisions. We restrict ourselves to central ( $b=0$ ) collisions of identical nuclei, when evidently the interaction area is  $\sigma_{AA}$ . The parameter  $\eta$  is then calculated according to (11). We have taken the string area  $\sigma_0$  as

$$\sigma_0 = \pi a^2, \quad a = 0.2 \text{ fm}. \quad (45)$$

in accordance with arguments presented in [7]. To relate the multiplicity to the experimental data we normalized  $\mu$  to the observable central (charged) multiplicity per unit rapidity in  $pp$  collisions at low energies. This fixes  $\mu_0$  for unit rapidity to be 1.1 The found values of  $\mu \equiv (dn^{ch}/dy)_{y=0}$  are presented in the Table for central S-S and Pb-Pb collisions (4d column) together with the corresponding values of c.m.energy  $\sqrt{s}$ ,  $\eta$  and number of strings  $N$  (1st to 3d columns, respectively). To compare, we present the values of  $\mu$  found without fusion and percolation (independent strings picture) in the 7th column. One should have in mind that the asymptotic formulas for the number

of collisions (42) - (44) used to determine the number of strings are not valid at comparatively low energies due to restrictions imposed by energy conservation. As stated in [1], at lower energies the number of collisions can be roughly obtained multiplying (42) - (44) by a factor 1/2. Correspondingly, our values for the multiplicity at two lower energies have to be corrected for energy conservation by a factor of this order. We preferred not to make this correction, since, in any case, it cannot be determined with any degree of rigour, and the effects we are considering are essential only at high enough energies, where (42)- (44) are hopefully valid.

As we observe, percolation considerably damps the multiplicity at high energies: at  $\sqrt{s} = 7000$  GeV for central Pb-Pb collision from nearly 8000 down to approximately 3000. This effect was predicted in our earlier papers on the string fusion [11,12] and is now reproduced in various models [17].

As to the FBC, we studied them both for the multiplicity and the inverse  $\langle p_T^2 \rangle$  (in fact for the observable  $\tau$ , defined in (41)). We have taken one half of the total rapidity available for the relevant rapidity window. The "external" dispersion in the denominator of (39) has to include also the fluctuations in the number of strings. We have assumed the overall distribution in  $N$  to be Poissonian so that  $\Delta N/N = 1/\sqrt{N}$ . As mentioned, for the multiplicity, due to its extensive character, the dispersion in  $N$  simply adds to  $D_C$ . It is large and absolutely dominates all other contributions. So it is no surprise that the coefficient  $b$  for the multiplicity with percolation (5th columns in the Table) only slightly differs from the one without percolation (8th column).

In contrast, for  $\tau$  the fluctuations in  $N$  only enter via the dependence of  $\eta$  on  $N$ . They result smaller than the percolation contribution at the maximum of the latter but fall with  $\eta$  more slowly, so that they dominate at large  $\eta$ . As a result, the characteristic peaked form of the parameter  $b$  found at fixed  $N$  (Fig. 5) disappears and  $b$  results steadily growing with  $\eta$  (6th column in the Tables). However one should note that in the independent string picture the parameter  $b$  for  $\tau$  is zero, since the dependence on  $N$  is then completely absent. So experimental study of the FBC for inverse  $\langle p_T^2 \rangle$  seems to be a promising way to observe signatures of string fusion and percolation.

## 6 Conclusions

In this study we have analyzed the impact of fusion and percolation of colour strings on global observables, such as multiplicities and  $\langle p_T^2 \rangle$ . To do this, a certain dynamical assumption has been made. The strings have been assumed to decay into the observed hadrons independently in each overlap.

On the qualitative level the results are best seen in the idealized case of a fixed number of strings  $N \gg 1$  (equivalent to plasma studies in the thermodynamic limit). A clear consequence of fusion and percolation is damping of the multiplicities, well described by a damping factor (15), which follows from the percolation theory. An unexpected but potentially important result is that the parameter  $b$  of the FBC shows a clear maximum at the percolation point. Such a maximum would be natural in fluctuations, say, of the cluster sizes, where it is to be expected as a signature of the percolation phase transition. However multiplicities do not seem to feel directly the cluster structure, so that the appearance of the maximum in their fluctuations is a new

result.

In the realistic case of nuclear collisions, where  $N$  fluctuates, the predicted multiplicities repeat the pattern observed at fixed  $N$  and are damped by the same factor (15). At the LHC energies it reduces the multiplicities by more than two times. However the parameter  $b$  for multiplicity results completely dominated by fluctuations in the number of strings and so only slightly different from the one in the independent string picture. A better (intensive) observable to see the impact of percolation is  $\langle p_T^2 \rangle$  or its inverse, for which the contribution of the fluctuations in  $N$  is drastically reduced. For  $\langle p_T^2 \rangle^{-1}$  we predict sizable values of  $b$  to be contrasted with  $b = 0$  in the independent string picture. Observation of nonzero values of  $b$  for  $\langle p_T^2 \rangle^{-1}$  would therefore be a clear signature of string fusion and percolation.

## 7 Acknowledgments

M.B. thanks the University of Santiago de Compostela for hospitality. C.P. thanks the Institute for Nuclear Theory of the University of Washington for hospitality. This study was supported by the NATO grant CRG.971461.

## 8 Appendix. Multiplicities and their dispersion

Let us recall the geometry of our percolation picture. Discs of radius  $a$  and area  $\sigma_0 = \pi a^2$  are homogeneously distributed in the total area  $S$ . It is assumed that centers of the discs are inside the unit circle of area  $S_0 = \pi$  so that  $S = \pi(1 + a)^2$ . The disc density is  $\rho = N/S$  and the percolation parameter is  $\eta = \rho\sigma_0 = N\sigma_0/S$ . In the thermodynamic limit  $N \rightarrow \infty$ , so that at fixed  $\eta$  the radius of the discs goes to zero. For fixed  $\eta$

$$a = \left( \sqrt{\frac{N}{\eta}} - 1 \right)^{-1}, \quad (46)$$

so that at large  $N$   $a \sim 1/\sqrt{N}$  and  $\sigma_0 \sim 1/N$ . Since the discs are distributed homogeneously, the probability that their centers are at points  $r_i$ ,  $i = 1, \dots, N$  inside the unit circle is independent of  $r_i$  and is given by

$$P(r_i) = S_0^{-N}. \quad (47)$$

Let us take a configuration which corresponds to the disc centers at points  $r_i$ . Then the overlap area of exactly  $n$  discs is given by the integral

$$S_n(r_1, \dots, r_N) = \int_S d^2r \sum_{\{i_1, \dots, i_n\} \subset \{1, \dots, N\}} \prod_{k=1}^n \theta(a - |\mathbf{r} - \mathbf{r}_{i_k}|) \prod_{k=n+1}^N \theta(|\mathbf{r} - \mathbf{r}_{i_k}| - a). \quad (48)$$

The average of  $S_N$  will be given by a multiple integral over  $r_i$  with the probability (47):

$$\langle S_n \rangle = \frac{1}{S_0^N} \int_{S_0} \prod_{i=1}^N d^2r_i S_n(r_1, \dots, r_N) = C_N^n \int_S d^2r F^n(r) (1 - F(r))^{N-n}, \quad (49)$$

where

$$F(r) = (1/S_0) \int_{S_0} d^2r_1 \theta(a - |\mathbf{r} - \mathbf{r}_1|). \quad (50)$$

The function  $S_0 F(r)$  gives an area occupied by a circle  $C$  of radius  $a$  with a center at  $r$  which is inside the unit circle  $S_0$ . If  $r < 1 - a$  then  $C$  is always inside  $S_0$  so that

$$F(r) = \sigma_0/S_0, \quad 0 < r < 1 - a. \quad (51)$$

However for  $r > 1 - a$  a part of  $C$  turns out to be outside the unit circle, and

$$F(r) = \sigma(r)/S_0, \quad 1 - a < r < 1 + a, \quad (52)$$

where  $\sigma(r) \leq \sigma_0$  is the overlap of the two discs  $C$  and  $S_0$ .

Generally, an overlap of two circles of radii  $r_1$  and  $r_2$  with a distance  $r$  between their centers is given by

$$\sigma(r_1, r_2, r) = (1/2)r_1^2(\alpha_1 - \sin \alpha_1) + (1/2)r_2^2(\alpha_2 - \sin \alpha_2), \quad (53)$$

where

$$\begin{aligned} \cos(\alpha_1/2) &= \frac{1}{2r_1} \left( r + \frac{r_1^2 - r_2^2}{r} \right), \\ \cos(\alpha_2/2) &= \frac{1}{2r_2} \left( r - \frac{r_1^2 - r_2^2}{r} \right). \end{aligned} \quad (54)$$

The function  $\sigma(r)$  in (52) is just  $\sigma(1, a, r)$ .

Formulas (49) -(54) allow to calculate numerically the average  $\langle S_n \rangle$  for any finite value of  $N$  without much difficulty.

In the thermodynamic limit,  $N \rightarrow \infty$  with  $\eta$  being fixed, the calculation of  $\langle S_n \rangle$  becomes trivial. Indeed then one can neglect the part of integration in  $r$  with  $r > 1 - a$  altogether, with an error  $\sim 1/a \sim 1/\sqrt{N}$ . With the same precision one then finds

$$\langle S_n \rangle = S C_N^n (\sigma_0/S)^n (1 - \sigma_0/S)^{N-n}, \quad (55)$$

where we have put  $S_0 \simeq S$ . The physically relevant values of  $n$  remain finite as  $N \rightarrow \infty$ . So we can approximately take

$$C_N^n = N^n/n!, \quad (1 - \sigma_0/S)^{N-n} = \exp(-N\sigma_0/S). \quad (56)$$

We then find that in the thermodynamic limit the distribution of overlaps in  $n$  is Poissonian with the mean value given by  $\eta$  (Eq. (13)).

Calculation of the multiplicity dispersion requires knowledge of the average of its square. With the centers of the discs at  $r_1, \dots, r_N$  it has the form

$$\mu^2(r_1, \dots, r_N) = (1/\sigma_0^2) \left( \sum_n \sqrt{n} S_n(r_1, \dots, r_N) \right)^2, \quad (57)$$

where  $S_N(r_1, \dots, r_N)$  is given by (48). Taking the average over the discs centers positions we now come to a double integral in  $r$  and  $r'$

$$\begin{aligned} \langle \mu^2 \rangle &= \frac{1}{\sigma_0^2} \sum_{m,n} \sqrt{mn} \int_S d^2r d^2r' \frac{1}{S_0^N} \int_{S_0} \prod_{i=1}^N d^2r_i \\ &\sum_{\{i_1, \dots, i_n\} \subset \{1, \dots, N\}} \prod_{k=1}^n \theta(a - |\mathbf{r} - \mathbf{r}_{i_k}|) \prod_{k=n+1}^N \theta(|\mathbf{r} - \mathbf{r}_{i_k}| - a) \end{aligned}$$

$$\sum_{\{j_1, \dots, j_m\} \subset \{1, \dots, i\}} \prod_{l=1}^m \theta(a - |\mathbf{r} - \mathbf{r}_{j_l}|) \prod_{l=m+1}^N \theta(|\mathbf{r} - \mathbf{r}_{j_l}| - a). \quad (58)$$

This complicated expression, however, continues to be factorized in all  $r_i$ . Let us assume for the moment that  $n \geq m$ . We can always rename the variables  $r_i$  to have in the first sum  $r_1, \dots, r_n$  as variables in the first product of  $\theta$ -functions (and as a result, the rest  $N - n$  variables  $r_{n+1}, \dots, r_N$  go into the second product). We shall then have  $C_N^n$  terms with the identical first sum. Now let  $p$  variables in the first product of  $\theta$ -functions in it coincide with  $p$  variables from the set  $r_1, \dots, r_n$ . We have  $C_n^p$  such terms, which will evidently all have the same dependence on the mentioned  $p$  variables. The left  $m - p$  variables from the first product of  $\theta$ -functions in the second sum do not coincide with any variables  $r_1, \dots, r_n$ , so they are chosen from variables  $r_{n+1}, \dots, r_N$ . We shall have  $C_{N-n}^{m-p}$  various terms of this sort. Thus the overall symmetry factor turns out to be a multibinomial coefficient

$$C_N^m C_N^p C_{n-n}^{m-p} = \frac{N!}{p!(n-p)!(m-p)!(n-n-m+p)!} \equiv C_N^{p, n-p, m-p}. \quad (59)$$

It multiplies the result of integration over all  $r_i$ ,  $i = 1, \dots, N$ , which has the form (at fixed  $r$  and  $r'$ )

$$\phi^p(r, r') \chi^{n-p}(r, r') \chi^{m-p}(r', r) \zeta^{N-n-m+p}(r, r'), \quad (60)$$

where

$$\begin{aligned} \phi(r, r') &= (1/S_0) \int_{S_0} \theta(a - |\mathbf{r} - \mathbf{r}_1|) \theta(a - |\mathbf{r}' - \mathbf{r}_1|), \\ \chi(r, r') &= (1/S_0) \int_{S_0} \theta(a - |\mathbf{r} - \mathbf{r}_1|) \theta(|\mathbf{r}' - \mathbf{r}_1| - a) = F(r) - \phi(r, r'), \\ \zeta(r, r') &= (1/S_0) \int_{S_0} \theta(|\mathbf{r} - \mathbf{r}_1| - a) \theta(|\mathbf{r}' - \mathbf{r}_1| - a) = 1 - F(r) - F(r') + \phi(r, r'), \end{aligned} \quad (61)$$

with  $F(r)$  defined before by (50). Of course one should sum over all possible values of  $p$ .

Combining all the terms, we find the expression for the average square of multiplicity as

$$\begin{aligned} \langle \mu^2 \rangle &= \frac{1}{\sigma_0^2} \sum_{n, m, p} \sqrt{(n+p)(n+p)} \\ &C_N^{n, m, p} \int_S d^2 r d^2 r' \phi^p(r, r') \chi^n(r, r') \chi^m(r', r) \zeta^{N-n-m-p}(r, r'). \end{aligned} \quad (62)$$

This expression is exact and may serve as a basis for the calculation of the average square of the multiplicity at finite  $N$ . However the new function  $\phi$  becomes very complicated when both variables  $r$  and  $r'$  are greater than  $1 - a$  (it is then given by the overlap area of three circles and we do not know any simple analytic expression for it).

For this reason rather than analyze the general expression (62) for finite  $N$  we shall immediately take the thermodynamic limit  $N \rightarrow \infty$ . We are in fact interested in the dispersion, not in the average square of multiplicity. It is important, since the leading terms in  $N$  cancel in the dispersion. So we shall study the difference

$$D^2 = \langle \mu^2 \rangle - \langle \mu \rangle^2 \quad (63)$$

in the limit  $N \rightarrow \infty$ ,  $\eta$  finite. As we shall see, although both terms in the right-hand side of (63) behave as  $N^2$  separately, their difference grows only as  $N$ .

Separating from (62) the term with  $p = 0$  and combining it with the second term on the right-hand side of (63) we present the total dispersion squared as a sum of two terms

$$D^2 = D_1^2 + D_2^2, \quad (64)$$

where

$$D_1^2 = \frac{1}{\sigma_0^2} \sum_{n,m} \sqrt{nm} \int_S d^2r d^2r' [C_N^{n,m} \chi^n(r, r') \chi^m(r', r) \zeta^{N-n-m}(r, r') - C_N^n C_N^m F^n(r) F^m(r') (1 - F(r))^{N-n} (1 - F(r'))^{N-m}] \quad (65)$$

and  $D_2^2$  is given by (62) with a restriction  $p \geq 1$ .

Function  $S_0\phi(r, r')$  gives the overlapping area of three circles: the unit circle  $S_0$  and two circles  $C$  and  $C'$  of radii  $a$  with centers at  $r$  and  $r'$ . It is evidently zero if  $R = |\mathbf{r} - \mathbf{r}'| > 2a$  since for such  $R$  circles  $C$  and  $C'$  do not overlap. Because of this, in the part  $D_2^2$ , which has at least one factor  $\phi$ , the integration in  $r$  and  $r'$  is restricted to the domain  $R < 2a$ , whereas in the part  $D_1^2$  the integration covers the whole range of values of  $R$ .

We begin with the part  $D_1^2$ . Splitting the integration region in  $r$  and  $r'$  in two parts,  $R > 2a$  and  $R < 2a$  we make use of (61) and present the first part as

$$D_{11}^2 = \frac{1}{\sigma_0^2} \sum_{n,m} \sqrt{nm} \int_{R>2a} d^2r d^2r' F^n(r) F^m(r') [C_N^{n,m} (1 - F(r) - F(r'))^{N-n-m} - C_N^n C_N^m (1 - F(r))^{N-n} (1 - F(r'))^{N-m}]. \quad (66)$$

One notices immediately that in the thermodynamic limit the leading terms in the integrand (independent of  $N$ ) cancel and only terms of the order  $1/N$  remain. The integration over  $r$  and  $r'$  provides a factor  $\propto N^2$  so that the total contribution results  $\propto N$ . To find this term we use that at large  $N$ , up to terms of the order  $1/N^2$ ,

$$C_N^n = \frac{N^n}{n!} \left( 1 - \frac{n(n-1)}{2N} \right),$$

$$C_N^{m,n} = \frac{N^{n+m}}{n!m!} \left( 1 - \frac{(m+n)(m+n-1)}{2N} \right),$$

$$(1 - F)^{N-n} = e^{-NF} (1 + nF - NF^2/2),$$

where we have taken into account that  $F$  has order  $1/N$ . Then we obtain

$$D_{11}^2 = \frac{1}{\sigma_0^2} \sum_{n,m} \frac{\sqrt{nm}}{n!m!} N^{n+m} \int_{R>2a} d^2r d^2r' F^n(r) F^m(r') \exp(-N(F(r) + F(r'))) (mF(r) + nF(r') - NF(r)F(r') - nm/N). \quad (67)$$

The integrand is now explicitly of the order  $1/N$ , so that we can change the integration region to  $r, r' < 1 - a$ , since the difference in the area will be of the order  $a^2 \sim 1/N$ , which results in the overall difference of the order  $1/N^2$  and can safely be neglected.

In the region  $r, r' < 1 - a$  both  $F(r)$  and  $F(r')$  are constants, given by (51). Integration over  $r$  and  $r'$  gives an overall factor  $S^2$ , so that in the end we get

$$D_{11}^2/N = \frac{1}{\eta^2} e^{-2\eta} \sum_{n,m} \frac{\eta^{n+m}}{n!m!} \sqrt{nm} [\eta(n+m) - \eta^2 - nm] = -\frac{(\eta\langle\sqrt{n}\rangle - \langle n\sqrt{n}\rangle)^2}{\eta^2}. \quad (68)$$

In the last expression the averages are to be taken over the Poissonian distribution with the mean value  $\eta$ . The part  $D_{11}^2$  is thus negative (and results comparatively small for all values of  $\eta$ ).

In the second part of  $D_1^2$  the integration goes over a small region  $R < 2a$ , of the order  $a^2 \sim 1/N$ , so that one can retain only the leading terms in the integrand. Passing to the integration over  $r$  and  $R$  one observes that at fixed  $r < 1 - a$  the integration region over  $R$  covers the whole region  $R < 2a$ . For  $r > 1 - a$  the integration region in  $R$  becomes much more complicated, determined by the condition  $r' = |\mathbf{r} + \mathbf{R}| < 1 + a$ . However the contribution from the latter region will be of the order  $a^3 \sim 1/N\sqrt{N}$ , since apart from a factor  $\propto a^2$  from the integration over  $R$ , a factor  $\propto a$  appears due to integration over  $r > 1 - a$ . So, up to terms of the relative order  $1/\sqrt{N}$ , we can neglect the contribution from the region  $r > 1 - a$ .

If  $r < 1 - a$  the circle  $C$  is completely inside the unit circle  $S_0$ . Then its intersection with the circle  $C'$  is also automatically inside  $S_0$ . Therefore function  $S_0\phi(r, r')$  in this region is simply given by the overlap of the circles  $C$  and  $C'$ , that is  $\sigma(a, a, R)$  defined by (53). We thus find

$$\phi(r, r') = \frac{\sigma_0}{S} \lambda(R), \quad (69)$$

where

$$\lambda(R) = (1/\pi)(\alpha - \sin \alpha), \quad \alpha = 2 \arccos(R/2). \quad (70)$$

Putting this into the expression for  $D_{12}^2$  and retaining the leading terms in the limit  $N \rightarrow \infty$  we obtain

$$D_{12}^2/N = \frac{2}{\eta} e^{-2\eta} \sum_{n,m} \frac{\sqrt{nm}}{n!m!} \eta^{n+m} \int_0^2 R dR [(1 - \lambda(R))^{n+m} e^{\eta\lambda(R)} - 1]. \quad (71)$$

This expression can be easily evaluated numerically. It is relatively large and also negative.

We finally come to the part  $D_2^2$ . The integration in  $r, r'$  goes over  $R < 2a$ , so that we can apply the same approximations as made in calculating  $D_{12}^2$ . We find

$$D_2^2/N = \frac{2}{\eta} e^{-2\eta} \sum_{n,m} \sum_{p=1} \frac{\sqrt{(n+p)(m+p)}}{n!m!p!} \eta^{n+m+p} \int_0^2 R dR \lambda^p(R) (1 - \lambda(R))^{n+m} e^{\eta\lambda(R)}. \quad (72)$$

This part is evidently positive. Its numerical evaluation shows that it nearly cancels the large negative contributions from  $D_1^2$  (in fact four digits are cancelled typically). So the numerical calculation of the dispersion requires some care.

## 9 References

- [1] A.Capella, U.P.Sukhatme, C.-I.Tan and J.Tran Thanh Van, Phys. Lett. **B81** 68 (1979); Phys. Rep. **236** 225 (1994).



- [2] A.B.Kaidalov and K.A.Ter-Martirosyan, Phys. Lett. **B117** 247 (1982).
- [3] B.Andersson, G.Gustafson and B.Nilsson-Almqvist, Nucl. Phys. **B281** 289 (1987).
- [4] K.Werner, Phys. Rep. **232** 87 (1993).
- [5] M.Gyulassy, CERN preprint CERN -TH 4794 (1987)
- [6] H.Sorge, H.Stoecker and W.Greiner, Nucl. Phys. **A498** 567c (1989).
- [7] N.Armento, M.A.Braun, E.G.Ferreiro and C.Pajares, Phys. Rev.Lett. **77** 3736 (1996).
- [8] M.A.Braun, C.Pajares and J.Ranft, Santiago de Compostela preprint US-FT/24-97, hep-ph/9707363.
- [9] M.Nardi and H.Satz, Bielefeld preprint BI-TP 98/10, hep-ph/9805297; H.Satz, Bielefeld preprint BI-TP 98/11, hep-ph/9805418.
- [10] T.S.Biro, H.B.Nielsen and J.Knoll, Nucl. Phys. **B245** 449 (1984).
- [11] M.A.Braun and C.Pajares, Phys. Lett. **B287** 154 (1992); Nucl. Phys. **B390** 542,549 (1993).
- [12] N.S.Amelin, M.A.Braun and C.Pajares, Phys. Lett. **B306** 312 (1993); Z.Phys. **C63** 507 (1994).
- [13] A.Bialas and W.Czyz, Nucl. Phys. **B267** 242 (1986) .
- [14] D.Stauffer, Phys. Rep. **54** 2 (1979).
- [15] M.B.Isichenko, Rev. Mod. Phys.**64** 961 (1992).
- [16] J.D.Bjorken, Phys.Rev **D 27** (1983) 140.
- [17] See e.g. A.Capella, A.Kaidalov and J.Tran Thanh Van, Orsay preprint LPT ORSAY 99-15, hep-ph/9903244.

## 10 Figure captions

Fig. 1. Projections of two overlapping strings onto the transverse plane.

Fig. 2. Damping of the multiplicity as a function of  $\eta$ .

Fig. 3. Percolation dispersion squared of the multiplicity per string in units  $\mu_0^2$  as a function of  $\eta$ .

Fig. 4. Fraction of the total interaction area covered by the maximal cluster as a function of  $\eta$ .

Fig. 5. Parameter  $b$  of the FBC for different rapidity intervals as a function of  $\eta$  for fixed  $N$ .

## 11 Table captions

Columns show from left to right: c.m. energy per nucleon  $\sqrt{s}$ ; parameter  $\eta$  (Eq. (1)); number of initially produced strings  $N$ ; central charged multiplicity per unit rapidity  $\mu$  and its FBC parameter  $B(\mu)$ , the FBC parameter for the inverse  $\langle p_T^2 \rangle$ ,  $b(\tau)$ , and the multiplicities and  $b(\mu)$  in the independent string model (subscript 0).

## 12 Table

**S-S scattering ( $b = 0$ )**

$\sqrt{s}$	$\eta$	$N$	$\mu$	$b(\mu)$	$b(\tau)$	$\mu_0$	$b_0$
19.4	0.33	99	101	0.67	0.04	111	0.65
62.5	0.47	143	140	0.74	0.08	160	0.72
200	0.65	198	185	0.79	0.13	221	0.77
546	0.84	255	228	0.82	0.18	284	0.80
1800	1.10	336	283	0.85	0.24	374	0.82
7000	1.47	448	349	0.87	0.30	499	0.85

**Pb-Pb scattering ( $b = 0$ )**

$\sqrt{s}$	$\eta$	$N$	$\mu$	$b(\mu)$	$b(\tau)$	$\mu_0$	$b_0$
19.4	1.45	1530	1200	0.69	0.13	1700	0.65
62.5	2.09	2200	1530	0.75	0.19	2450	0.72
200.0	2.88	3040	1870	0.78	0.25	3390	0.77
546.0	3.72	3920	2170	0.80	0.28	4370	0.80
1800.0	4.90	5170	2530	0.81	0.31	5760	0.82
7000.0	6.53	6890	2940	0.82	0.33	7680	0.85

13 Figures

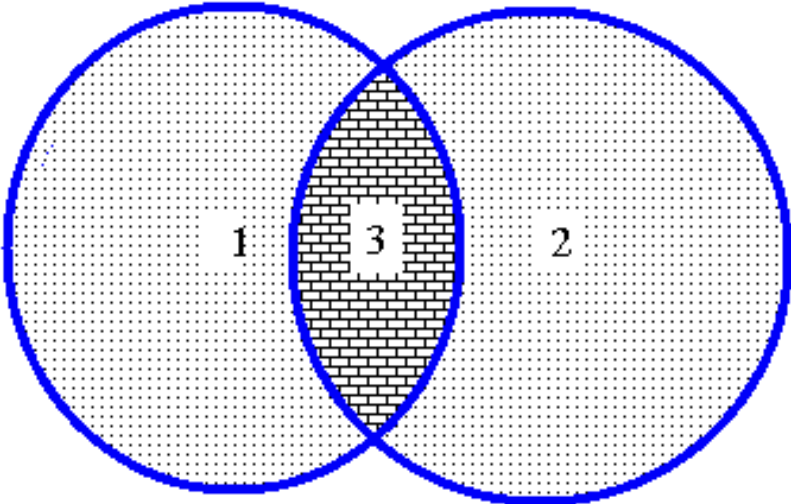


Figure 1: Projections of two overlapping strings onto the transverse plane.

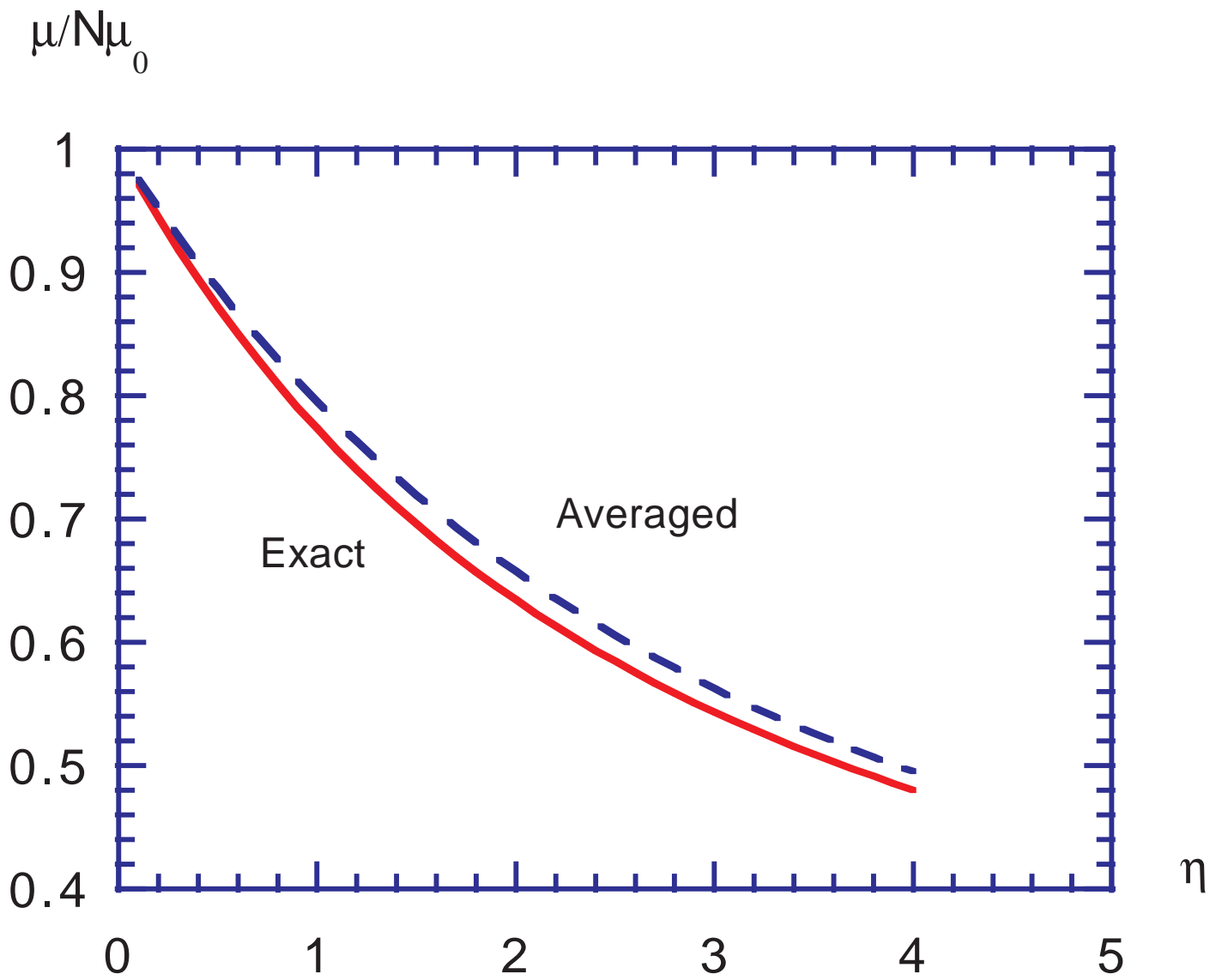


Figure 2: Damping of the multiplicity as a function of  $\eta$ .

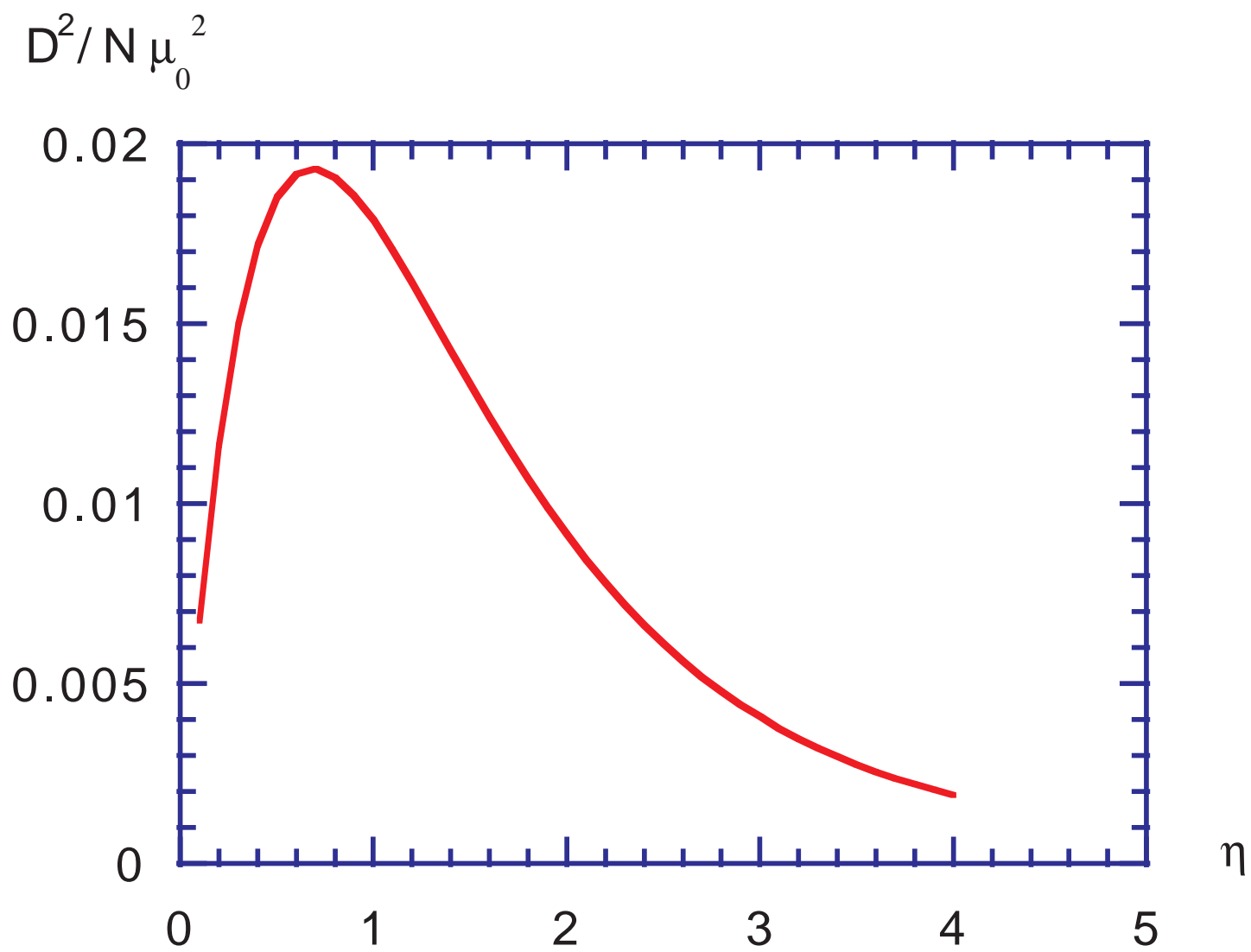
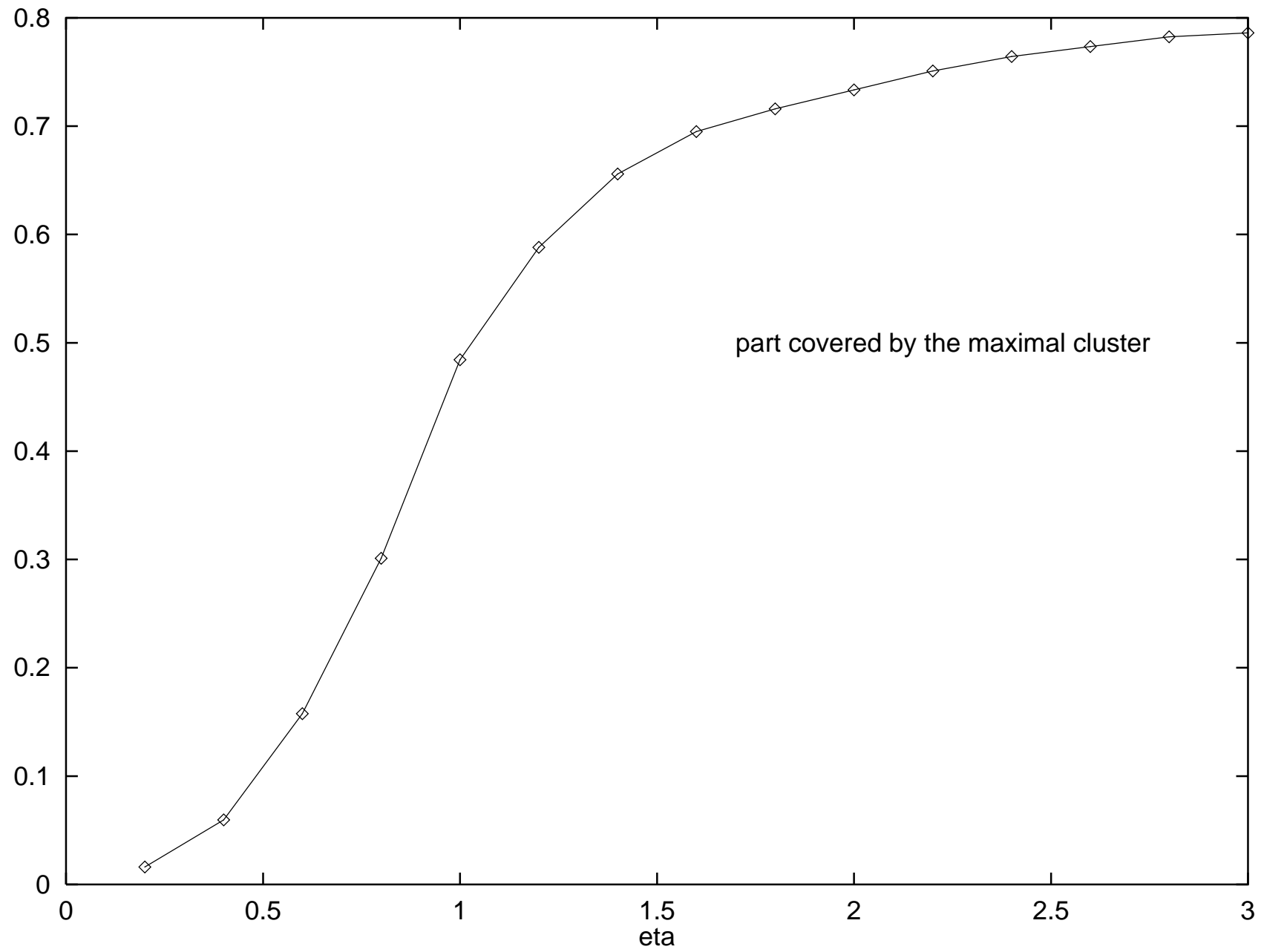


Figure 3: Percolation dispersion squared of the multiplicity per string in units  $\mu_0^2$  as a function of  $\eta$ .

Figure 4: Fraction of the total interaction area covered by the maximal cluster as a function of  $\eta$



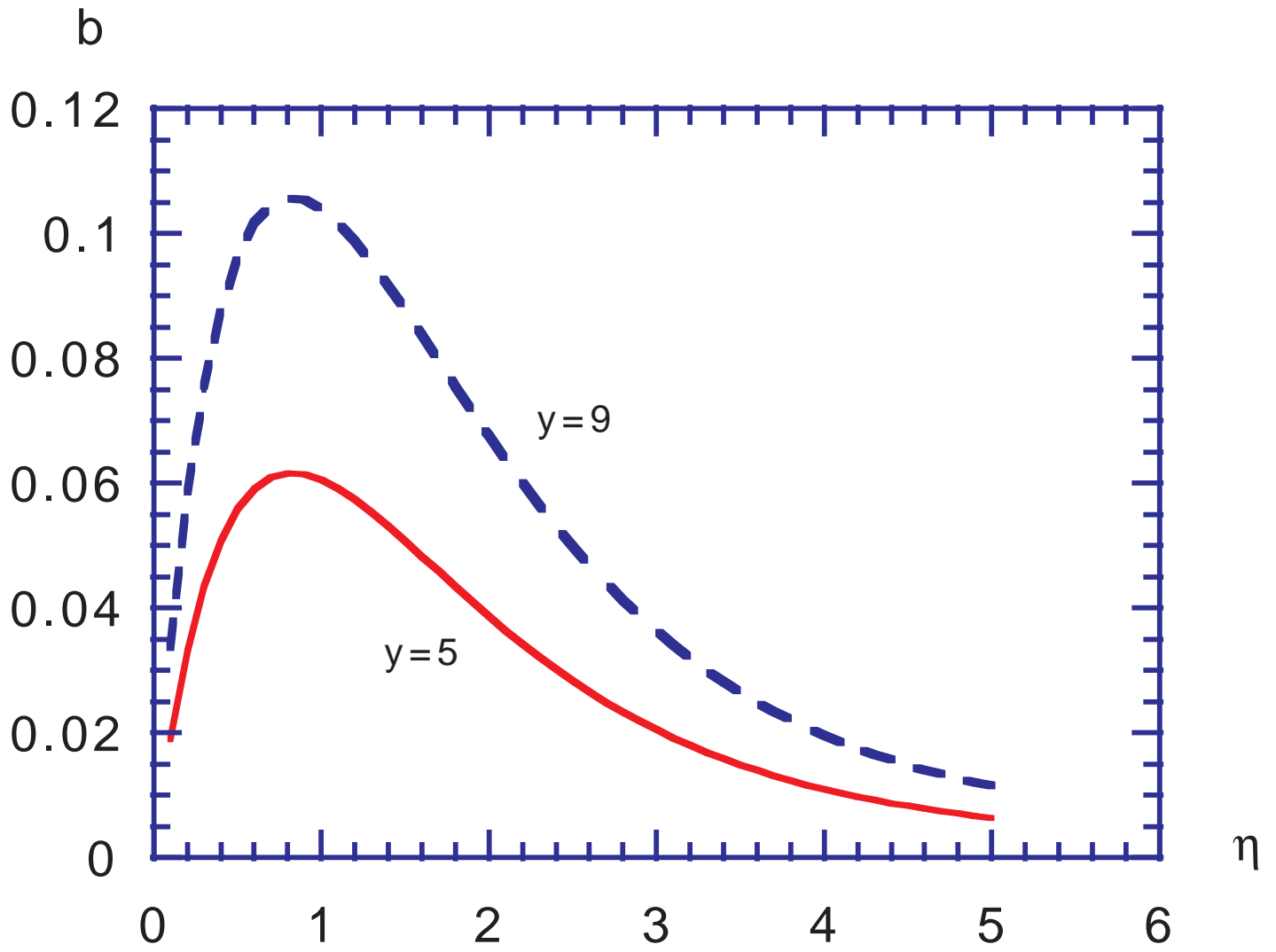


Figure 5: Parameter  $b$  of the FBC for different rapidity intervals as a function of  $\eta$  for fixed  $N$ .